

See discussions, stats, and author profiles for this publication at: <https://www.researchgate.net/publication/30929912>

Effect of Ion Bombardment and Annealing on the Electrical Properties of Hydrogenated Amorphous Silicon Metal–Semiconductor–Metal Structures

Article in *Journal of Applied Physics* · February 2005

DOI: 10.1063/1.1834710 · Source: OAI

CITATIONS

12

READS

181

4 authors, including:



Julius Orwa

La Trobe University

49 PUBLICATIONS 944 CITATIONS

[SEE PROFILE](#)



Robert Gateru

Riara University

5 PUBLICATIONS 17 CITATIONS

[SEE PROFILE](#)



S Ravi P Silva

University of Surrey

682 PUBLICATIONS 14,188 CITATIONS

[SEE PROFILE](#)

Some of the authors of this publication are also working on these related projects:



Diamond and DLC thin films [View project](#)



Molecular materials and naphthalic imides [View project](#)

Effect of ion bombardment and annealing on the electrical properties of hydrogenated amorphous silicon metal–semiconductor–metal structures

J. O. Orwa,^{a)} J. M. Shannon, R. G. Gateru, and S. R. P. Silva

Advanced Technology Institute, School of Electronics and Physical Sciences, University of Surrey, Guildford, Surrey GU2 7XH, United Kingdom

(Received 20 August 2004; accepted 21 October 2004; published online 27 December 2004)

The electrical properties of hydrogenated amorphous silicon (*a*-Si:H) metal–semiconductor–metal (MSM) devices are investigated as a function of Si bombardment dose prior to and after annealing. We observe that conduction in unbombarded devices is surface-barrier controlled whereas it is bulk controlled in bombarded devices. The resistance decreases with bombardment dose in a manner consistent with increased hopping conductivity in highly damaged structures. A relative permittivity of between 8 and 12, depending on dose, was calculated from experimental Poole–Frenkel plots for bombarded devices. These values compare closely with the theoretical relative permittivity for amorphous silicon of 11.7 and confirm that conduction is by Poole–Frenkel mechanism. For bulk-controlled conduction, we observe an increase in the zero-field Coulombic trap barrier height with decreasing dose, ranging from 0.53 for a Si dose of $5 \times 10^{13} \text{ cm}^{-2}$ to 0.89 for a dose of $2 \times 10^{12} \text{ cm}^{-2}$. We attribute this to a decrease in the concentration of charged defects with decreasing dose and find that the change in concentration of charged centers needs to be about $4 \times 10^{19} \text{ cm}^{-3}$ to account for the change of 0.35 eV from the lower to the upper dose. Activation energies obtained from Arrhenius plots of current density against temperature varied with dose and temperature in a similar way as Coulombic barrier height. We explain these results in terms of the variation in the number of charged defect centers with dose and annealing temperature and a shift in the Fermi level. © 2005 American Institute of Physics. [DOI: 10.1063/1.1834710]

I. INTRODUCTION

Following the initial investigations on chalcogenide glasses¹ in the early 1960s, reversible switching has been studied in a variety of thin-film materials including nickel oxides,² amorphous silicon,³ hydrogenated amorphous silicon⁴ and, more recently, hydrogenated amorphous (silicon-rich) silicon carbide.^{5,6} A typical switching device consists of a thin-film material sandwiched between two metal contacts, forming a metal–semiconductor–metal (MSM) or metal–insulator–metal (MIM) device. A suitable voltage pulse applied to the top contact of the device causes a transition from a high to a low resistance state in a process called forming. Once formed, the device can be switched back and forth between the two states by applying a slightly lower voltage pulse of alternating polarity. A prerequisite in the practical application of MSM structures as switching devices is reproducibility in forming voltages and on-resistances. Research has shown that this can be achieved by introducing defects *by design* into the MSM structure prior to forming. Techniques such as current stressing⁷ and doping⁵ have been used in the past to introduce defects. Ion-beam bombardment, more recently used, produces dangling bonds, which form defect states in the band gap of the semiconductor material. This study examines the electrical properties, prior to forming, of a thin film of hydrogenated amorphous silicon (*a*-Si:H) sandwiched between Cr contacts, with glass as the substrate. The film was bombarded with Si to a range

of doses and patterned into $200 \times 200\text{-}\mu\text{m}^2$ -size devices, thus allowing a study of the electrical properties as a function of dose.

Unlike most previous bombardment work^{8,9} where low-energy ions were used to damage the top metal–semiconductor (MS) interface region as a way of modifying the Schottky barrier, we have implanted Si deep into the middle of the *a*-Si:H layer so that the damage extends to within the bulk of the active region. This is intended to ensure that both the Schottky barrier and bulk transport properties are affected. By self-implanting Si, we eliminate any chemical effects so that any changes in conductivity of the device are due only to damage created in the form of dangling bonds and not as a result of doping. Information gained from this study will be useful in explaining some of the postforming electronic switching behavior of these devices.

II. EXPERIMENTAL PROCEDURE

A layer of Cr, 100 nm thick, was sputtered on a $2 \times 2\text{-in.}$ glass substrate to form the back contact. On this was deposited a 70-nm layer of *a*-Si:H by plasma-enhanced chemical-vapor deposition (PECVD) ($\text{SiH}_4\text{-}320^\circ\text{C}$) followed by 150 nm of insulating SiN deposited by reactive ion sputtering of silicon in a nitrogen atmosphere. The resulting structures were ion-beam bombarded by 30-keV Si at doses of 2×10^{12} , 5×10^{12} , and $5 \times 10^{13} \text{ cm}^{-2}$. The bombardment energy was chosen so that the end of the range was roughly in the middle of the *a*-Si:H layer. Finally, a 60-nm Cr layer was sputtered to make the top contact. Appropriate masks were used with each layer deposition to create hundreds of

^{a)}Author to whom correspondence should be addressed; electronic mail: j.orwa@surrey.ac.uk

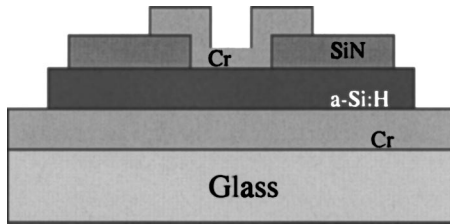


FIG. 1. A cross-sectional view of the samples studied showing the different layers.

devices with dimensions of $200 \times 200 \mu\text{m}^2$ on the 2×2 -in. glass substrate. A cross-sectional view through the structures studied is shown in Fig. 1. Current-density–voltage (J – V) measurements were first carried out on as-deposited devices using a computer-controlled Keithley 236 Source-Measure unit. Samples were then furnace annealed in a nitrogen environment for 30 min at 423, 473, 523, 573, and 623 K and allowed to cool down to room temperature following each annealing before recording the J – V data. Activation energies were deduced from the temperature-dependent J – V data.

III. RESULTS AND DISCUSSION

Figure 2 shows the J – V plots for the unbombarded and devices bombarded with Si at 2×10^{12} , 5×10^{12} , $5 \times 10^{13} \text{ cm}^{-2}$ doses. The asymmetry observed in the J – V spectra between the positive and negative biases in the unbombarded sample indicates that the conduction is Schottky barrier controlled. From the magnitude of the saturated current density at zero electric field, the Schottky barrier heights for the unbombarded sample are approximately 0.90 and 0.84 eV for the top and bottom contacts, respectively. In addition to the asymmetry, the unbombarded device displays the least current. For the bombarded devices, Fig. 2 and 3 show that there is a progressive increase in current and J – V curve symmetry with dose. It is well known that long-range disorder in amorphous materials causes the abrupt band edges typical of crystalline materials to be replaced by a broadened tail of states extending from the conduction and valence bands into the band gap. The degree of extension of

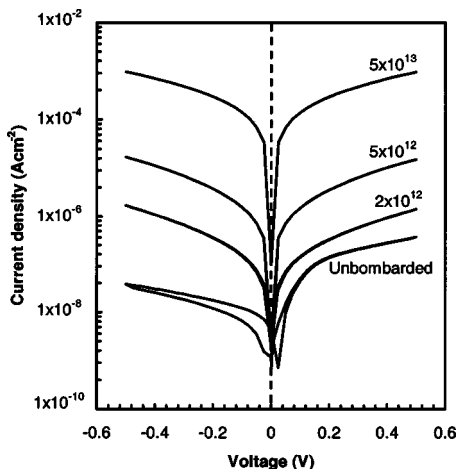


FIG. 2. J – V curves for unbombarded device and devices bombarded with Si at doses of 2×10^{12} , 5×10^{12} , and $5 \times 10^{13} \text{ cm}^{-2}$. The obvious asymmetry seen for the unbombarded device is absent in the bombarded samples.

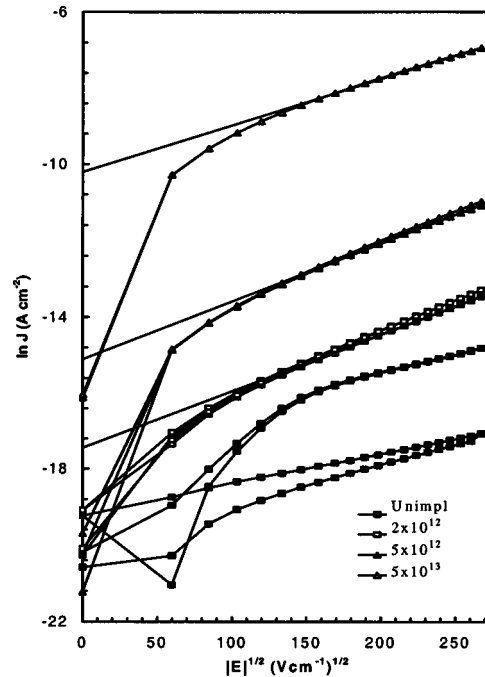


FIG. 3. Poole–Frenkel plots showing an increase in current and symmetry with dose.

these tail states into the forbidden gap indicates the strength of the band tails and is proportional to the concentration of weak silicon–silicon bonds. For bombarded materials, an increase in dose increases bond-length and bond-angle disorder as well as concentration of weak silicon–silicon bonds, which are manifested as an increase in the strength of the band tails. Furthermore, the broadening of the band tails results in an increase in the concentration of silicon dangling bonds, many of which are charged. As previously noted,^{8,10} the increase in current and symmetry with dose can be attributed to an increase in the density of defects in the bulk of the a -Si:H. These changes, in particular, the increase in J – V symmetry, indicate that the introduction of defect states changes the conduction mechanism from Schottky barrier to bulk controlled.

The large amount of damage created when the a -Si:H is bombarded with Si suggests that bulk conduction could be by hopping between defects via a Poole–Frenkel-type mechanism. The Poole–Frenkel effect is the thermal emission of charge carriers from Coulombic traps in the bulk of a dielectric or semiconductor, enhanced by the application of an electric field, which lowers the surface-barrier height on one side of the trap, thereby increasing the probability of the electron escaping from the trap. The Poole–Frenkel current density is given by¹¹

$$J = J_0 \exp\left(-\frac{q\phi_t - \beta\sqrt{E}}{\xi kT}\right), \quad (1)$$

where E is the applied electric field, q the electron charge, and ϕ_t is the zero-field Coulombic trap barrier height. The parameter ξ in the denominator fluctuates between 1 and 2 depending on the level of damage.¹² The Poole–Frenkel coefficient, β , is related to the dielectric constant, ϵ_r , of the material and is expressed as

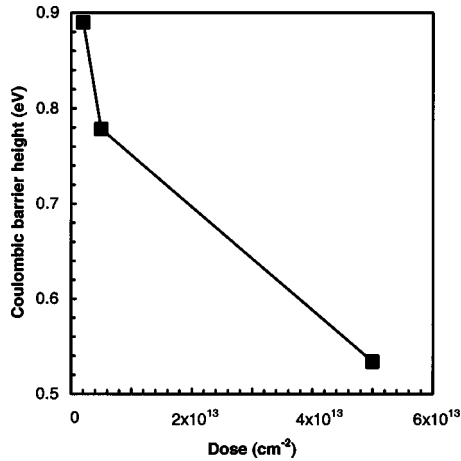


FIG. 4. Coulombic barrier height vs dose showing a decrease in the barrier height as dose increases.

$$\beta = \sqrt{\frac{q^3}{\pi\epsilon_0\epsilon_r}}, \quad (2)$$

where ϵ_0 is the permittivity of free space. Equation (1) predicts an increase in current with increasing field due to the effective reduction in the ionization potential, ϕ_t , by $\beta\sqrt{E}$. In order to determine if conduction is by the Poole–Frenkel mechanism, Eq. (1) may be rewritten as

$$\ln J = \frac{\beta}{\xi kT} \sqrt{E} + \left(\ln J_0 - \frac{q\phi_t}{\xi kT} \right). \quad (3)$$

A plot of the natural logarithm of J against \sqrt{E} (see Fig. 3) reveals near-perfect symmetry in the curves as dose increases, indicating a shift from Schottky barrier to bulk-controlled conduction via Poole–Frenkel mechanism. By using Eqs. (2) and (3) we have extracted a relative permittivity of 12.7 for the $5 \times 10^{13} \text{ cm}^{-2}$ Si dose sample and values of 8.9 and 8.6 for the 5×10^{12} and $2 \times 10^{12} \text{ cm}^{-2}$ Si dose samples, respectively. For the unbombarded sample, Eqs. (2) and (3) give a relative permittivity of 24.1. This is an unrealistic result which, together with the lack of J – V curve symmetry between positive and negative biases, indicates that conduction in unbombarded devices is not by the Poole–Frenkel mechanism. The close agreement between our experimental relative permittivity for bombarded a -Si:H and the theoretical result of 11.7, together with the excellent symmetry in the J – V curves for the bombarded samples, on the other hand, confirms that conduction in these highly damaged structures is by the Poole–Frenkel mechanism.

Figure 4 shows that as dose increases, the Coulombic barrier height (ϕ_t) decreases, ranging from a value of 0.89 V at a dose of $2 \times 10^{12} \text{ cm}^{-2}$ down to 0.53 V at a dose of $5 \times 10^{13} \text{ cm}^{-2}$. There are three possible explanations for these variations: a change in the Fermi level, a change¹² of the Poole–Frenkel coefficient, or the presence of high concentrations of charged defects. Since the material is undoped and silicon bombardment does not introduce donors or acceptors, it is unlikely that there is much change in the position of the Fermi level with bombardment dose. Furthermore, in a highly damaged nonequilibrium material, the Fermi level should be near the center of the band gap. Defect complexes

such as those involving oxygen do introduce donors⁸ but the oxygen content would need to be extremely high to shift the Fermi level over the range needed to account for the change of the Coulombic barrier. Similarly the change in the Poole–Frenkel coefficient¹² is not sufficient to explain these effects. It therefore seems likely that the reduction in barrier height is due to the presence of a large concentration of charged defects.

It can be shown¹³ that a charged defect in the vicinity of a center emitting a carrier will lower the barrier by an amount inversely proportional to the separation between the two centers as

$$\Delta E_{A0} = \frac{q^2}{\pi\epsilon_0\epsilon_r r_a}, \quad (4)$$

where r_a is the distance between the centers. Thus, knowing r_a , the associated change in the charge density can be calculated. Since the average separation is proportional to the cube root of the number of charged defects ($N_{CD}^{-1/3}$), the change of barrier height decreases rapidly with increasing dose as is indeed seen in Fig. 4. From Eq. (4) we find that the concentration of charged centers needs to be about $4.1 \times 10^{19} \text{ cm}^{-3}$ to account for the change of 0.35 eV from a bombardment of 2×10^{12} to $5 \times 10^{13} \text{ cm}^{-2}$ Si dose. Since each ion has an energy of 30 keV and most of the slowing down is via atomic displacements with a threshold energy of ~ 25 eV, there will always be a large cascade of displacements per ion. We calculate that for a dose of $4.8 \times 10^{13} \text{ cm}^{-2}$, every atom in the layer ($\sim 5 \times 10^{22} \text{ cm}^{-3}$) is displaced at least once. It is therefore easy to generate a defect density of $4.1 \times 10^{19} \text{ cm}^{-3}$.

Large concentrations of charged defect states are not unexpected in a -Si:H since dangling-bond states are amphoteric and, as predicted by the defect pool model,^{14,15} these states can be positively or negatively charged or neutral. In equilibrium the net charge will be zero but, following bombardment, the distribution of dangling-bond states will be well away from equilibrium. Annealing up to the equilibration temperature (~ 240 °C in a -Si:H) will, however, remove excess dangling-bond defect states leaving behind a residual disorder, which depends on the original damage.¹⁰ This residual disorder determines the distribution of the remaining dangling-bond states and the strength of the band tails.

Figure 5 shows the room temperature J – V data for the sample implanted with $5 \times 10^{13} \text{ cm}^{-2}$ Si dose following annealing at 423, 473, 523, 573, and 623 K. The samples were cooled to room temperature before recording the J – V curves. With the increase in annealing temperature, we note a decrease in the current density and an increase in the asymmetry of the J – V curves, indicative of the recovery of the structure towards the reference unbombarded state. However, some residual damage always remains and the reference curves cannot be fully recovered for the temperature range investigated. As shown in Fig. 6, the dependence of the Coulombic barrier height on annealing temperature below 523 K is not very uniform for the different doses. While the lowest-dose sample shows a decrease in this temperature region, the highest dose shows an increase and the intermediate dose

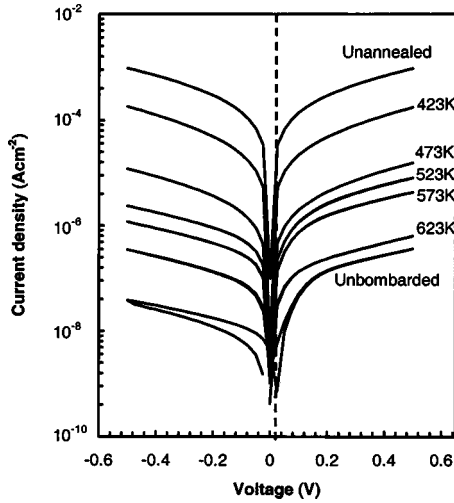


FIG. 5. J - V curves showing a decrease in current density with annealing temperature. The curve labeled unannealed was implanted with $5 \times 10^{13} \text{ cm}^{-2}$ Si but not annealed. As the annealing temperature increases, the J - V curves become asymmetric and shift towards the unbombarded reference, indicating a partial recovery of the structure.

displays a fluctuating value. The decrease in Coulombic barrier height with annealing temperature is unusual and we attempt an explanation below when we address the activation energy results. Between 573 and 623 K the activation energy increases for all samples studied. In all cases, however, the barrier height decreases with dose at all annealing temperatures in a similar manner, as shown in Fig. 4. The increase in the barrier height with temperature can be explained in terms of defect density as was done for dependence of Coulombic barrier height on dose. Annealing causes a reduction in the number of defects and increases their separation. As separation between centers gets larger we expect the current to drop as the probability of hopping from center to center decreases, which could explain the observed increase in the Coulombic barrier height with annealing temperature.

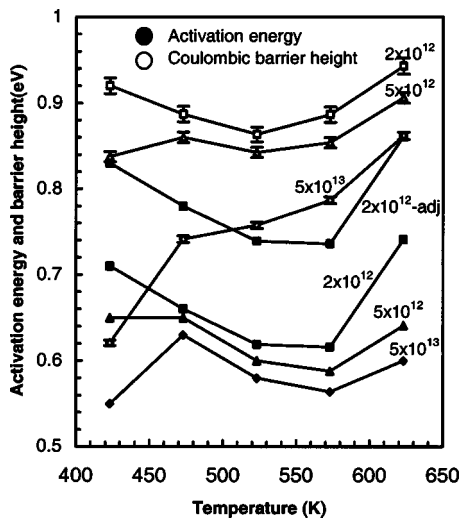


FIG. 6. Dependence of Coulombic barrier height (open markers) and activation energy (filled markers) on annealing temperature. After adjusting the activation energy by adding $\beta\sqrt{E}$ (curve labeled 2×10^{12} -adj), the results are closer together. The labels on the curves refer to Si bombardment dose (ions cm^{-2}).

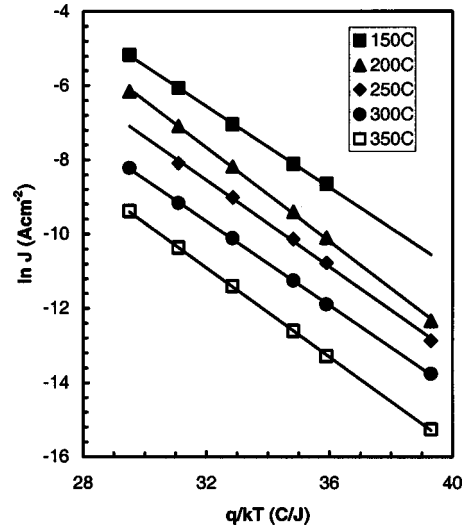


FIG. 7. Arrhenius plots of current density against temperature.

To verify our Coulombic barrier height results, we have performed J - V measurements at various temperatures and extracted the activation energy from the Arrhenius plots of current density against temperature (see Fig. 7) according to the equation

$$J = A \exp\left(-\frac{qE_A}{kT}\right). \tag{5}$$

In Eq. (5), J is the current density, E_A the activation energy, k the Boltzmann constant, and T the ambient temperature in Kelvin. The activation energies (filled markers) are plotted in Fig. 6 to allow comparison with the Coulombic barrier height (open markers). In general, the activation energies obtained from Eq. (5) are lower than the corresponding Coulombic barrier heights derived from the Poole-Frenkel equation because the latter is obtained by extrapolating to zero electric field whereas the activation energy was measured at 2 V. After adjusting the values for the activation energy by adding $\beta\sqrt{E}$, the results are closer together (see adjusted data for 2×10^{12} Si dose in Fig. 6) and can be made to nearly coincide by the addition of a further constant. What this implies is a scaling factor that is not field dependent, but possibly dictated by either geometric or physical conditions. The similarity in the dose and temperature variation of the Coulombic barrier height and the activation energy shows that conduction in these bombarded devices indeed occurs by hopping in a manner consistent with the Poole-Frenkel mechanism. The observed decrease in both the Coulombic barrier height and the activation energy with dose is an indication that the large number of defects created at higher doses causes the density of hopping centers to increase.

The initial decrease in activation energy with annealing temperature observed in Fig. 6 is anomalous. One would expect the decrease in current with annealing temperature observed in Fig. 5 to be due either to a fall in the concentration of hopping centers or an increase in the activation energy or both. In a highly damaged nonequilibrium material, such as is the case after bombardment and prior to annealing, the Fermi level should be near the center of the band gap.

Annealing generally causes passivation of defects and so we expect a fall in the number of hopping centers as partial recovery of the preimplantation structure is achieved. This recovery should push the Fermi level closer to its intrinsic value and this manifests itself as a higher activation energy as observed for temperatures above 500 K. Yet, the data clearly show a drop in both activation energy and Coulombic barrier height between 420 and 520 K. Taken together with the lower conduction shown in Fig. 5, it could mean that at low annealing temperatures, defects are initially redistributed prior to being passivated. The ordering at low temperatures could cause the decrease in activation energy while defect passivation at higher temperatures would push the Fermi level towards the band edge as well as increase the distance between hopping centers. The overall result would be an increase in activation energy and Coulombic barrier height as observed.

IV. SUMMARY

Electrical properties of *a*-Si:H MSM devices have been investigated as a function of bombardment dose and annealing temperature. We find that conduction in unbombarded devices is Schottky barrier controlled whereas it is bulk controlled in bombarded devices. For bulk-controlled conduction, we observe a decrease in the zero-field Coulombic trap barrier height with increasing dose, which we attribute to the diminishing interdefect separation as the number of hopping centers increases with dose. The close agreement between

our experimental relative permittivity and the theoretical result suggests that bulk conduction is by Poole–Frenkel mechanism. This is confirmed by the similarity in dose and temperature variation between Poole–Frenkel-derived Coulombic barrier heights and activation energies obtained from Arrhenius plots. The decrease in activation energy with decreasing current is anomalous and could be due to a shift in the Fermi level towards the band edge.

ACKNOWLEDGMENT

The authors wish to thank EPSRC for sponsoring this research through a Portfolio Partnership grant.

- ¹S. R. Ovshinsky, Phys. Rev. Lett. **21**, 1450 (1968).
- ²J. F. Gibbons and W. E. Beadle, Solid-State Electron. **7**, 785 (1964).
- ³C. Feldman and K. Moorjani, Thin Solid Films **5**, R1 (1970).
- ⁴M. C. Gabriel and D. Adler, J. Non-Cryst. Solids **48**, 297 (1982).
- ⁵J. M. Shannon and S. P. Lau, Electron. Lett. **35**, 1976 (1999).
- ⁶R. G. Gateru, J. M. Shannon, and S. R. P. Silva, Mater. Res. Soc. Symp. Proc. **742**, k.2.3 (2003).
- ⁷J. Hu, A. J. Snell, J. Hajto, and A. E. Owen, Philos. Mag. B **80**, 29 (2000).
- ⁸J. M. Shannon and C. H. Chua, Solid-State Electron. **47**, 1903 (2003).
- ⁹M. K. Chai, J. M. Shannon, and B. J. Sealy, Electron. Lett. **34**, 919 (1998).
- ¹⁰R. A. C. M. M. van Swaaij, A. D. Annis, B. J. Sealy, and J. M. Shannon, J. Appl. Phys. **82**, 4800 (1997).
- ¹¹A. K. Johscher, J. Electrochem. Soc. **116**, 217C (1969).
- ¹²S. P. Lau, J. M. Shannon, and B. J. Sealy, J. Non-Cryst. Solids **227–230**, 533 (1998).
- ¹³J. M. Shannon and A. D. Annis, Philos. Mag. Lett. **72**, 323 (1995).
- ¹⁴S. C. Deane and M. J. Powell, Phys. Rev. B **48**, 10815 (1993).
- ¹⁵M. J. Powell and S. C. Deane, Phys. Rev. B **53**, 10121 (1996).